ISSN 2075-1087, Gyroscopy and Navigation, 2015, Vol. 6, No. 1, pp. 33–40. © Pleiades Publishing, Ltd., 2015.
Published in Giroskopiya i Navigatsiya, 2014, No. 3, pp. 41–52.

Sensitivity Limits of Coupled Resonator Optical Waveguide (CROW) Gyroscopes when Subject to Material Losses

D. Kalantarov and C. Search

Department of Physics and Engineering Physics, Stevens Institute of Technology, Hoboken, USA
e-mail: DKalanta@stevens.edu, CSearch@stevens.edu

Received July 15, 2014

Abstract—In recent years there has been a growing interest in optical microresonators as viable low cost on chip micro-optical gyroscopes with navigation grade sensitivities. Here, we analyze and compare the rotational sensitivity of coupled resonator optical waveguide (CROW) gyroscopes to equivalent single resonator gyroscopes under various geometric constraints and device parameters. We show that the CROW gyros offer a sensitivity enhancement over conventional single resonator gyros at low propagation losses. However, the single ring resonator gyro is found to be more stable over a wider range of propagation losses as well as boasting greater sensitivities for larger propagation losses compared to a CROW of the same size. Furthermore, an analysis of the maximum achievable sensitivity for different material technologies (Hydex, silicon oxynitride, and SOI) is conducted. While all materials achieved tactical grade sensitivities, Hydex shows the greatest potential for CROW gyros because of the stability of its sensitivity over a wide range of device parameters.

DOI: 10.1134/S2075108715010058

INTRODUCTION

Over the past decade, there has been a growing interest in integrated optical gyroscopes in order to usher in a new generation of low cost on chip micro-optical gyroscopes with navigation grade sensitivities. However, to achieve such sensitivities in an integrated device a complete redesign of current optical gyroscopes is needed. Both ring laser gyroscopes (RLGs) and fiber optic gyroscopes (FOGs) have become a mainstay for inertial navigation due to their simplicity, robustness, and superior sensitivities (down to 0.001 deg/h) compared to mechanical gyroscopes. Despite their success, RLGs and FOGs are unsuitable for small portable devices because of their large size and weight. By contrast, MEMS (micro-electromechanical systems) gyroscopes have been able to reduce the overall footprint to that of a commonplace microchip. However, the best MEMS gyroscopes only have sensitivities which are at least three orders of magnitude below the sensitivity needed for inertial navigation. A variety of different designs for both active and passive integrated optical gyroscopes have been proposed [1, 2]. Such microphotonic gyroscopes have dimensions comparable to MEMS gyroscopes (10–100 mm^2) with theoretical sensitivities significantly exceeding MEMS and approaching their much larger siblings RLGs and FOGs. Moreover, microphotonic gyroscopes, like MEMS, can be fabricated on semiconductor chips using standard fabrication technology but, unlike MEMS, they have no moving parts making them easier to fabricate and in principle more robust. Such devices may potentially satisfy the need for low cost on chip gyroscopes for high sensitivity applications such as hand held navigation in GPS denied regions [1].

Among the different types of integrated optical gyros that have been proposed, passive arrays of coupled optical microresonators have shown promise [3–12]. Specifically, coupled resonator optical waveguides (CROWs) [13], which consist of a linear array of evanescently coupled ring resonators, have been investigated for their potential as micro-optical gyroscopes [6–9]. However, there has been much debate over whether such arrays of sequentially coupled microresonators do indeed have sensitivities exceeding that of individual resonators with the same size as the CROW [4–7]. This paper aims to evaluate and compare the maximum achievable sensitivity, defined as the minimum detectable angular rotation rate in degrees per hour (deg/h), of an N resonator CROW gyro and a single ring resonator gyro for various material propagation losses, size constraints, and coupling coefficients. We show that in fact CROW gyros offer a sensitivity enhancement over conventional single resonator gyros at low propagation losses. However, the single resonator gyros have sensitivities that are more stable over a wide range of propagation losses.

To our knowledge a CROW gyroscope has not yet been fabricated nor has there yet been a study of the achievable sensitivities for commonly used material platforms: Hydex glass, silicon oxynitride (SiON), and silicon on insulator (SOI) [13]. We find that, although SOI is one of the most widely used materials for CROW devices, it has the lowest achievable sensitivity due to its very high propagation losses. However, the other materials were able to achieve sensitivities sufficient for tactical

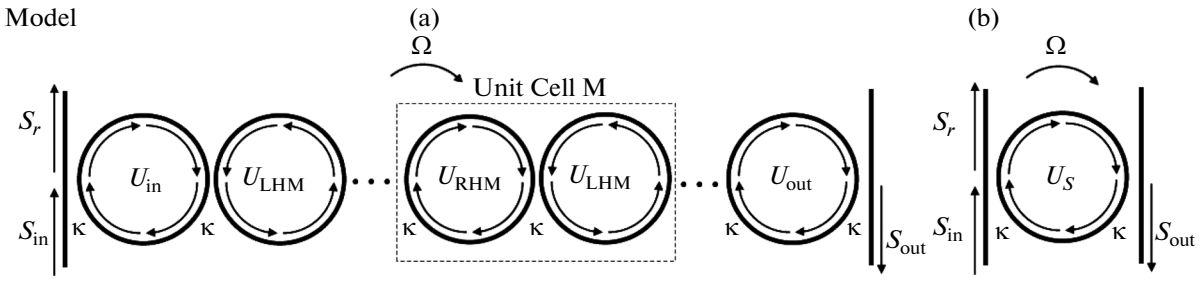

Fig. 1. (a) Microring CROW gyroscope of N resonators coupled to waveguides and (b) equivalent single ring resonator showing the relationship between the resonators and transfer matrices defined in the text. s_{in} and s_{out} are the input and transmitted fields such that the transmission is $T(\phi_s) = |s_{out}/s_{in}|^2$. Based on the propagation direction of s_{out}, the number of resonators must be odd due to phase matching.

grade sensing with dimensions comparable to that of typical MEMS devices. Finally, looking beyond existing materials, we calculate for fixed geometric areas, chosen to be comparable to commercially available MEMS gyroscopes, the maximum permissible propagation losses capable of achieving rate, tactical, and inertial grade rotation sensitivities.

MODEL

To analyze the transmission through the rotating CROW we utilize the transfer matrix [14, 15] approach developed in [7–9]. As a result of momentum conservation, the propagating right handed mode (RHM) of one resonator couples to the counter propagating left handed mode (LHM) of the adjacent resonator and vice versa. Consequently, transmission can be expressed in terms of input (U_{in}), output (U_{out}), LHM (U_{LHM}), and RHM (U_{RHM}) transfer matrices which represent the coupling between the input waveguide and first resonator, the coupling between the last resonator and output waveguide, and the repetitive unit cell of the CROW shown in Fig. 1, respectively. These matrices as well the transfer matrix for a single ring resonator are:

$$U_{in} = \frac{-i}{\sqrt{\kappa}}\begin{pmatrix} \sqrt{1-\kappa}\,e^{i(\phi_p+\phi_s)} & -e^{i(\phi_p+\phi_s)} \\ e^{-i(\phi_p+\phi_s)} & -\sqrt{1-\kappa}\,e^{-i(\phi_p+\phi_s)} \end{pmatrix}, \quad (1)$$

$$U_{out} = \frac{1}{\kappa}\begin{pmatrix} \sqrt{1-\kappa}\,e^{i(\phi_p+\phi_s)} & -e^{-i(\phi_p+\phi_s)} \\ e^{i(\phi_p+\phi_s)} & -\sqrt{1-\kappa}\,e^{-i(\phi_p+\phi_s)} \end{pmatrix} \times \begin{pmatrix} \sqrt{1-\kappa} & -1 \\ 1 & -\sqrt{1-\kappa} \end{pmatrix}, \quad (2)$$

$$U_{RHM} = \frac{-i}{\sqrt{\kappa}}\begin{pmatrix} \sqrt{1-\kappa}\,e^{i(\phi_p+\phi_s)} & -e^{i(\phi_p+\phi_s)} \\ e^{-i(\phi_p+\phi_s)} & -\sqrt{1-\kappa}\,e^{-i(\phi_p+\phi_s)} \end{pmatrix}, \quad (3)$$

$$U_{LHM} = \frac{i}{\sqrt{\kappa}}\begin{pmatrix} \sqrt{1-\kappa}\,e^{i(\phi_p-\phi_s)} & -e^{i(\phi_p-\phi_s)} \\ e^{-i(\phi_p-\phi_s)} & -\sqrt{1-\kappa}\,e^{-i(\phi_p-\phi_s)} \end{pmatrix}, \quad (4)$$

$$U_S = \frac{1}{\kappa}\begin{pmatrix} (1-\kappa)e^{i(\phi_p+\phi_s)} - e^{-i(\phi_p+\phi_s)} & -\sqrt{1-\kappa}\left(e^{i(\phi_p+\phi_s)} - e^{-i(\phi_p+\phi_s)}\right) \\ \sqrt{1-\kappa}\left(e^{i(\phi_p+\phi_s)} - e^{-i(\phi_p+\phi_s)}\right) & (1-\kappa)e^{-i(\phi_p+\phi_s)} - e^{i(\phi_p+\phi_s)} \end{pmatrix}, \quad (5)$$

where $\phi_p = \beta\pi R$ is half the roundtrip propagation phase for a resonator of radius R with propagation constant $\beta = \omega n/c - i\alpha/2$ for light of angular frequency ω. The effective index of refraction is n while α is the power attenuation coefficient per unit length [9, 16]. κ is the dimensionless coupling between resonators, $0 < \kappa \le 1$, which represents the fraction of the power coupled out of a resonator and is expressible in terms of an overlap integral between the mode functions in adjacent resonators or resonator and waveguide [17]. The coupled cavity waveguide transmission matrix for a signal propagating from the left to right waveguide for a CROW and equivalent single ring resonator is respectively given as:

$$T_{CROW} = U_{out}\left(U_{LHM}U_{RHM}\right)^M U_{LHM}U_{in} = \begin{pmatrix} T_{11} & T_{12} \\ T_{21} & T_{22} \end{pmatrix}, \quad (6)$$

$$T_{Ring} = U_S = \begin{pmatrix} T_{11} & T_{12} \\ T_{21} & T_{22} \end{pmatrix},$$

where $M = (N - 3)/2$. The transmission function, which is proportional to the output power, is $T(\phi_s) = |T_{11}T_{22} - T_{21}T_{12}|^2/|T_{22}|^2$ which reduces to $|T_{22}|^2$ in the

limit of $\alpha = 0$ such that all transfer matrices are unimodular.

When the CROW is rotated about an axis perpendicular to the plane of the device at the angular rate Ω, the Sagnac effect leads to a nonreciprocal phase shift between light propagating in the clockwise (right handed modes, RHM, in Fig. 1) and counterclockwise (left handed modes, LHM, in Fig. 1) direction around each resonator. Assuming a clockwise inertial rotation of the resonators, the clockwise propagating wave acquires upon one full revolution around a resonator the Sagnac phase ϕ_S while the counter-clockwise wave acquires the phase $-\phi_S$, where the phase shift is defined in terms of the rotation rate as $\phi_S = 2\pi\omega\Omega R^2/c^2$.

The gyroscope scale factor, S, which measures the sensitivity to rotations, relates the change in the transmission to a small change in the inertial rotation rate, $\delta T = S\delta\Omega$, and is expressed as [4–9, 18, 19],

$$S = \frac{1}{P_{\text{in}}}\frac{dP_{\text{out}}}{d\Omega} = \frac{dT}{d\Omega} = \left(\frac{2\pi\omega R^2}{c^2}\right)\left(\frac{dT}{d\phi_s}\right), \qquad (7)$$

where $P_{\text{out}} = TP_{\text{in}}$ is the optical power at the device output in terms of the input power. In this study, three types of amplitude noise, quantum shot noise, thermal current noise in the photodetector, and laser intensity noise are taken into account in order to calculate the minimum detectable angular rate, Ω_{min}. We ignore phase noise due to the laser source linewidth under the assumption that the effective length of the CROW, $L_{\text{eff}} = N\pi R/\kappa$ is less than the laser coherence length. The minimum detectable rotation Ω_{min} is found when the scale factor is a maximum such that $S_{\max}\Omega_{\min}$ equals the relative noise fluctuations in the photodetector [7, 19, 20],

$$\Omega_{\min} = \frac{1}{S_{\max}}\sqrt{\left(\frac{e}{i_D} + \frac{4k_BT'}{R_Li_D^2} + RIN\right)\Delta f}. \qquad (8)$$

Here $i_D = (e\eta\lambda/hc)P_{\text{out}}$ is the photodetector current, $\Delta f = 1$ Hz is the measurement bandwidth, P_{out} is the maximum power incident onto the photodetector, $R_L = 50\Omega$ is the assumed photodetector load resistance, T is temperature chosen to be 298 K, RIN is the relative intensity noise of the laser and was chosen to be -160 dB/Hz [20], e is the fundamental electric charge, and $\eta = 1$ the quantum efficiency of the photodetector [1, 20]. At low incident power (<100 pW) the thermal noise is the dominant noise however at high incident power (>2 mW) the system becomes dominated by laser noise. All results presented here use a source wavelength of $\lambda = 1.55$ μm, and an input power of 1 mW, where shot noise is the dominant source of noise.

CROWs based on SiON, Hydex glass, and SOI have been routinely fabricated and used for studying linear device applications including filters and delay lines as well as for studying nonlinear wave mixing [21]. From the perspective of optical propagation through microresonators, these material platforms are differentiated in terms of the losses per unit length, α, in the waveguides comprising the resonators and the index of refraction contrast, Δn, between the resonator waveguides and the cladding material. A larger Δn reduces the minimum bending radius of the waveguides enabling not only a smaller device footprint but also a larger free spectral range of the resonators. However, a larger Δn increases the sensitivity to fabrication inaccuracies, such as sidewall roughness which induces higher losses and backreflections [22]. SOI consisting of silicon resonators ($n \approx 3.5$) embedded in silica ($n \approx 1.5$) has the largest index contrast $\Delta n_{\text{SOI}} = 140\%$ [19, 23] but also the largest losses, $\alpha_{\text{SOI}} = 0.8$–$3$ dB/cm [24]. Silicon oxynitride has the smallest index change $\Delta n_{\text{SiON}} = 4.5\%$ [22, 25] with lower losses, $\alpha_{\text{SiON}} = 0.15$–$0.35$ dB/cm [22, 26]. Hydex glass by far has the smallest losses $\alpha_{\text{Hydex}} = 0.06$ dB/cm [27, 28] with $\Delta n_{\text{Hydex}} = 14\%$ [28, 29]. Moreover, the cited values of Δn correspond to minimum bending radii of approximately 300 μm for SiON [25, 26], 40 μm for Hydex [28, 29] and, 5–6 μm for SOI [30, 31]. We do not consider here polymer resonators made of PMMA despite being a common material for CROWs since propagation losses are greater than SOI amounting to larger roundtrip losses than the other three materials [21]. PMMA is therefore the least desirable material.

RESULTS

Resolution requirements for various gyroscope classes

	Rate grade	Tactical grade	Inertial grade
$\lvert\delta\Omega\rvert$, deg/h	>300	300 to 29	<0.6

Table, adapted from [20], summarizes the resolution requirements for three classes of inertial sensing applications. Applications such as video game controllers or camera stabilization would be classified under rate grade while inertial navigation, usually the domain of RLGs, would fall under inertial grade. Tactical grade would correspond to military applications such as guided weapons.

Initially a sensitivity comparison between CROW gyros with N resonators confined to a fixed geometric area and a single resonator with the same area, $N(\pi R^2)$, was conducted, see Fig. 2. An inter-resonator coupling of $\kappa = 0.1$, corresponding to spacing between resonators of several hundred nanometers, and a cross-sectional width of 1 μm for the resonator waveguides were chosen. Areas were chosen to be 5 mm^2, 50 mm^2, and 100 mm^2, which are comparable to commercially available MEMS gyros. Figure 2a shows the sensitivity of the CROW and single resonator of equal area for the lossless case, $\alpha = 0$ dB/cm, where one sees that Ω_{min} is inversely proportional to

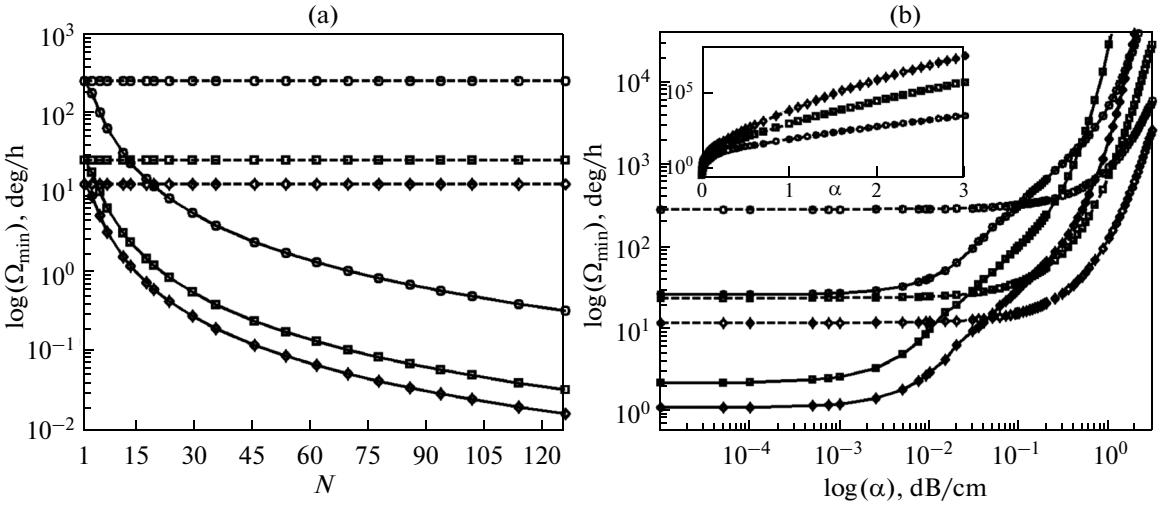

Fig. 2. (a) Ω_{min} vs. N for lossless resonators and (b) Ω_{min} vs. α for $N = 15$ constrained to an area of 5 mm^2 (lines with circles), 50 mm^2 (lines with squares) and 100 mm^2 (lines with diamond). Inset shows the ratio of Ω_{min} with and without losses for the CROW gyro. Solid lines are CROW gyros and dashed lines are single resonators of equal area both for $\kappa = 0.1$.

the geometric area of both devices as expressed in Eq. (7). Since no loss is assumed in the CROW structure, maximizing the number of resonators by using the smallest possible resonators leads to the best sensitivity. Note that since the total area of the CROW is fixed implying that R decreases with increasing N. Additionally the sensitivity of the single resonator is always worse than the CROW for all N. For the CROW, the enhanced sensitivity is the result of optical interference between the signal propagating in different resonators [6]. This leads to a sharpening of the slope at the edges of the CROW's transmission band as N increases [6]. In fact, a numerical data fit for the values of S_{max} vs. N shows that for $N \gg 1$, S_{max} is proportional to N^4 when $\alpha = 0$. Thus, in the case of 15 resonators the CROW has an order of magnitude increase in sensitivity over the single ring resonator, while at ≈60 resonators there is a two order of magnitude increase over the single resonator when confined to the same geometric area.

Figure 2b examines the effects of propagation loss on the maximum sensitivity in a CROW gyro with 15 resonators and a single ring resonator confined to the same area. It is evident from Fig. 2b. that for low losses, $\alpha < 10^{-2}$ dB/cm, the $N = 15$ CROW yields a nearly order of magnitude better sensitivity than the single resonator of equal area. However, the single ring resonator gyro's sensitivity is substantially more stable to changes in α over a wider range of values as well as boasting greater sensitivities for $\alpha \geq 0.1$ dB/cm than the CROW device. For example, when confined to an area of 50 mm^2, the sensitivity of an 15 resonator CROW becomes an order of magnitude worse than for no losses when $\alpha = 0.025$dB/cm while the sensitivity of a single resonator of the same area becomes an order of magnitude worse than the lossless case when $\alpha =$ 0.6 dB/cm. Similarly, an $N = 15$ CROW and a single resonator gyro of equal area of 100 mm^2 with $\alpha =$ 0.3 dB/cm produces $\Omega_{min} = 238$ and 56 deg/h, respectively.

In order to understand the increased performance of the single resonator when subject to large losses, we recall that the transmission band of the CROW as a function of ϕ_s consists of N closely spaced transmission resonances as shown in Fig. 3 [6]. For a lossless CROW the maximum slope of the transmission always occurs at the edges of the transmission band and yields the maximum scale factor. However, in the presence of resonator losses, represented by propagation loss, α, signal attenuation leads to a lowering of each of the resonances, which becomes more pronounced the higher α is, subsequently reducing the transmission slopes and hence the scale factor. Moreover, the transmission resonances at the band edges are significantly more reduced as α increases than is the case for the central resonance, ultimately shifting the location of maximum slope and also scale factor inward away from the edge, see Fig. 4. This shift in the location of the maximum transmission slope from the edge to the central resonance corresponds to the abrupt reduction in sensitivity seen in Fig. 2b as α is increased. By contrast, the single ring has only a single transmission resonance as a function of ϕ_s, which is less sensitive to changes in α than the CROW band edges. Owing to the resonance's much higher tolerance to propagation loss, the single ring's scale factor is less affected by losses than the CROW.

Additionally a study of how κ and the number of resonators, N, affect Ω_{min} for various materials, Hydex, SiON, and SOI, when confined to a maximum geometric area of 5 and 50 mm^2 was conducted, see Fig. 4. All have R greater than the minimum material

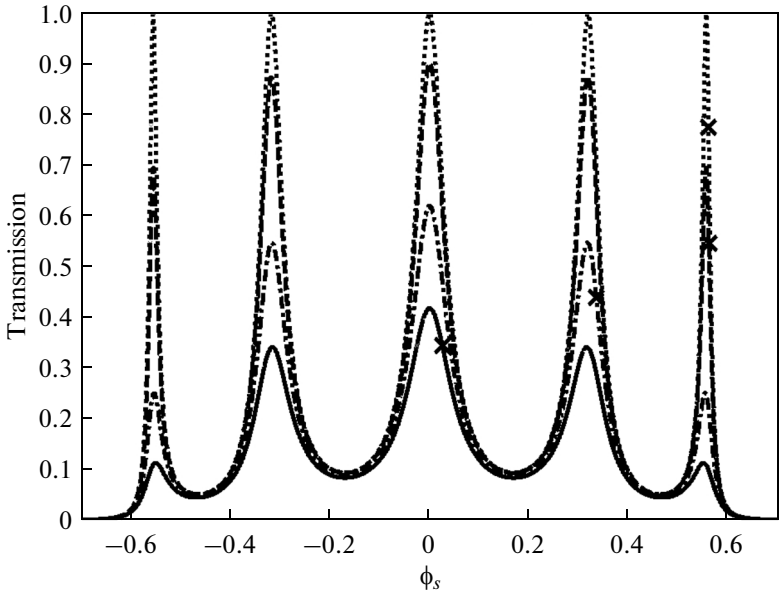

Fig. 3. Transmission $T(\phi_s)$ of an N= 5 CROW gyro for $\alpha = 0$ dB/cm (dotted line), $\alpha = 0.1$ dB/cm (dashed line), $\alpha = 0.5$ dB/cm (dot-dashed line), and $\alpha = 1$ dB/cm (solid line). Crosses represent the location of the maximum scale factor. Here $\kappa = 0.1$ and device area was fixed at 5 mm^2.

bending radius along as well as having cross-sectional widths of the resonator waveguides of 0.5 μm for SOI, 2.2 μm for SiON, and 1.5 μm for Hydex. The results indicate that the maximum sensitivity occurs for the smallest value of κ in the range of $0.1 < \kappa < 1$. Moreover, it is evident from Fig. 4 that increasing the device area leads to increased sensitivities. These two conclusions are true for all of the configurations except SOI confined to an area of 50 mm^2. Since light circulates on average $1/2\kappa$ times in each resonator leading to an effective device length of $L_{\text{eff}} = N\pi R/\kappa$, propagation losses lead to an exponential reduction in the transmission by an amount that is approximately $\exp(-\alpha L_{\text{eff}})$. As either N or R increase, the exponential transmission reduction eventually becomes more significant than the increase in sensitivity due to more N or larger size. This not only causes a shift of the maximum scale factor location inward from the band edge but also a decrease in the sensitivity for further increases in N or R, as in the case of SOI with area of 50 mm^2.

Furthermore, for larger values of κ, the minimum achievable value of Ω_{min} not only becomes larger but also occurs at larger values of N. Upon comparison of the three materials in Fig. 4 it is clear that all three have the potential for tactical grade sensitivity. However, only Hydex glass was able to attain this while being confined to the smaller of the two areas, 5 mm^2. Moreover, SOI technology with the larger propagation losses limits the maximum sensitivities to at best rate-grade. Although, currently available technologies and device constraints put inertial grade sensitivities out of reach, Hydex has emerged as a potentially promising platform for the development of low cost tactical-grade CROW gyros. Its low propagation losses and the limited number of required resonators make it an ideal candidate. Furthermore, Hydex confined to an area of 50 mm^2 is able to maintain its tactical grade sensitivity over an extremely wide range of N and κ values ranging from 3–29 and 0.1 to 0.95, respectively. For instance, the minimum value of Ω_{min} for $\kappa = 0.1$ in Fig. 4d occurs at 3 resonators with $\Omega_{\text{min}} = 31$ deg/h while for $\kappa = 0.95$ at 29 resonators the minimum is $\Omega_{\text{min}} = 79$ deg/h which is less than a 3x decrease in sensitivity and still within tactical range.

Looking beyond the three materials discussed so far, we evaluate the permissible losses and number of resonators that are able to achieve the three grades of sensitivity listed in Table I. The values of α and N as well as the associated resonator radii needed to achieve rate, tactical, and inertial grade sensitivities for devices constrained to an area of 4 mm^2 is shown in Fig. 5a where κ was chosen to be 0.1. The number of resonators were varied from 1 to 125 corresponding to radii of 1200–90 μm. The solid and dot-dashed lines with square markers correspond to the values of N and α needed to achieve $\Omega_{\text{min}} = 300$ deg/h and $\Omega_{\text{min}} = 29$ deg/h, respectively. These lines mark the boundary between rate and tactical grade sensitivity and the lower bound of tactical grade sensitivity, respectively. Consequently, any combination of resonator number and propagation loss above the $\Omega_{\text{min}} = 300$ deg/h curve will yield rate grade sensitivities while values between the $\Omega_{\text{min}} = 300$ deg/h and $\delta\Omega_{\text{min}} = 29$ deg/h lines have tactical grade sensitivities. The dot-dashed line with diamond markers shows the values of N and α yielding

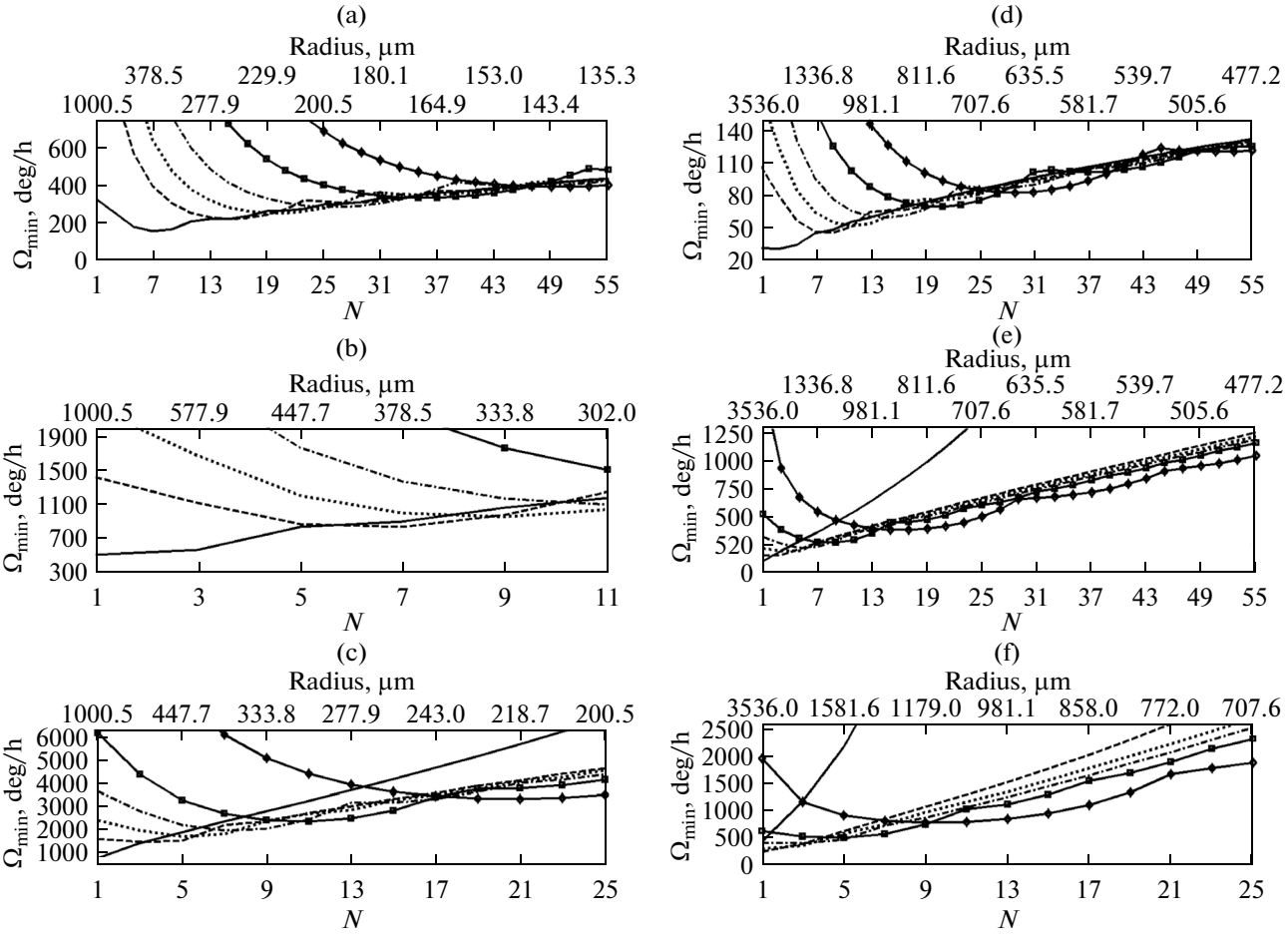

Fig. 4. Ω_{min} vs. number of resonators, N, for the following CROWs: (a) Hydex ($\alpha_{Hydex} = 0.06$ dB/cm) with device area of 5 mm^2; (b) SiON ($\alpha_{SiON} = 0.15$ dB/cm) with device area of 5 mm^2; (c) SOI ($\alpha_{SOI} = 0.8$ dB/cm) with area 5 mm^2; (d) Hydex ($\alpha_{Hydex} = 0.06$ dB/cm) with area 50 mm^2; (e) SiON ($\alpha_{SiON} = 0.15$ dB/cm) with area 50 mm^2; and (f) SOI ($\alpha_{SOI} = 0.8$ dB/cm) with area 50 mm^2. Resonator couplings are $\kappa = 0.1$ (solid lines), $\kappa = 0.35$ (dashed lines), $\kappa = 0.5$ (dotted lines), $\kappa = 0.65$ (dot-dashed lines), $\kappa = 0.8$ (solid likes with squares), and $\kappa = 0.95$ (solid lines with diamonds).

$\Omega_{min} = 0.6$ deg/h, which represents the upper bound for inertial grade sensitivities. Any combination of α and N below the line will result in inertial grade sensitivities. Similarly Fig. 5b demonstrates the different combinations of N and values of α needed to maintain $\Omega_{min} = 300$ deg/h, for CROWs confined to maximum geometric areas of 5, 50, and 100 mm^2. Values of N and α below each curve have tactical grade sensitivities for each device size.

Our analysis indicates that for a fixed geometric area, as the number of resonators increases the maximum permissible propagation losses decreases, potentially narrowing the range of materials to be used. Furthermore, each contour of fixed Ω_{min} exhibits a certain number of resonators where the allowable losses reach a maximum. For instance with an area 5 mm^2 and $\Omega_{min} = 29$ deg/h, the permissible propagation loss is maximum at $N = 17$ having the value $\alpha = 0.0018$ dB/cm. Finally, as seen in Fig. 5b, increasing the device size for a fixed Ω_{min}, the maximum allowable propagation loss shifts upwards and towards $N = 1$ in agreement with our earlier conclusion that for large losses the single resonator gyro is more sensitive than the equal size CROW.

CONCLUSIONS

In conclusion it was found that in the lossless case, a CROW gyro with N resonators confined to a fixed geometric area has better sensitivity for any value of $N > 1$ than a single resonator gyro of equal area. Moreover, maximizing the number of resonators by using the smallest possible resonators leads to the best sensitivity. However, in the presence of resonator losses it was found that the single ring resonator gyro's sensitivity is substantially more stable to a wide range of propagation losses compared to the CROW gyro of the same size. Furthermore, as propagation losses

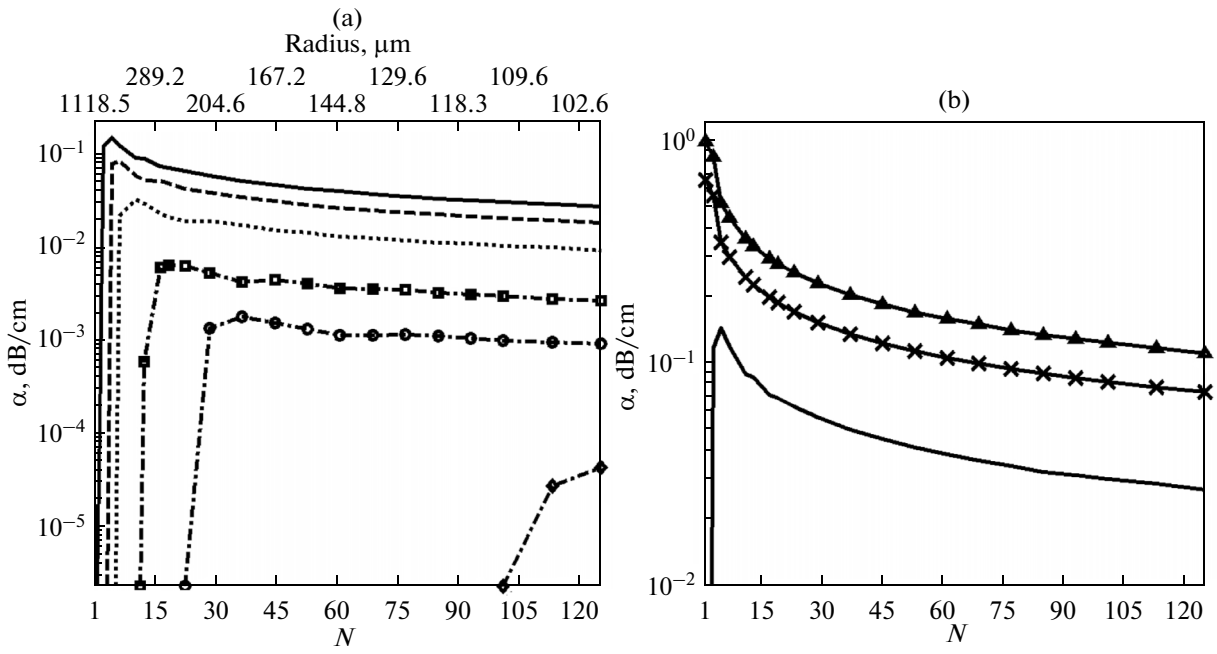

Fig. 5. Propagation loss, α, and number of resonators, *N*, required to achieve the following sensitivities Ω_{min} = 300 deg/h (solid line), Ω_{min} =200 deg/h (dashed line) , Ω_{min} =100 deg/h (dotted lines), Ω_{min} =29 deg/h (dot-dashed line with squares), Ω_{min} = 10 deg/h (dot-dashed line with circles), and Ω_{min} = 0.6 deg/h (dot-dashed line with diamonds) for (a) geometric area of 4 mm^2 and (b) Ω_{min} =300 deg/h for geometric area 4 mm^2 (solid line), 50 mm^2 (solid line with x's), and 50 mm^2 (solid line with triangles). In all cases κ = 0.1.

increase the single ring system begins to boast greater sensitivities than the CROW system.

Our analysis of various materials found that Hydex has the greatest potential for the development of tactical-grade CROW gyros due to its ability to achieve tactical grade sensitivities over a very wide range of resonator numbers and couplings. In general, in order to fabricate gyroscopes with inertial grade sensitivities and with dimensions comparable to MEMS gyros, a material with ultra-low propagation losses as well as a large number of resonators will need to be used. However, it is important to note that in practice it may be extremely difficult to fabricate the extensive number of resonators required to achieve the desired sensitivities, while maintaining uniformity of the resonator circumferences and inter-resonator coupling. Such disorder will have the effect of degrading the overall sensitivity.

REFERENCES

1. Ciminelli, C., Dell'Olio, F., Campanella, C.E., and Armenise, M.N., Photonic technologies for angular velocity sensing, *Adv. Opt. Photon.*, 2010, no. 2, pp. 370–404.
2. Passaro, V., de Tullio, C., Troia, B., Notte, M., Giannoccaro, M., and Leonardis, F., Recent Advances in Integrated Photonic Sensors, *Sensors*, 2012, no. 12, pp. 15558–15598.
3. Scheuer, J. and Yariv, A., Sagnac effect in coupled-resonator slow-light waveguide structures, *Phys. Rev. Lett.*, 2006, vol. 96, p. 053901.
4. Terrel, M.A., Digonnet, M.J.F., and Fan, S., Performance limitation of a coupled resonant optical waveguide gyroscope, *J. Lightwave Technol.*, 2009, vol. 27, pp. 41–46.
5. Terrel, M.A., Digonnet, M.J.F., and Fan, S., Performance comparison of slow-light coupled-resonator optical gyroscopes, *Laser & Photon. Rev.* 2009, vol. 3, pp. 452–465.
6. Kalantarov, D. and Search, C.P., Effect of input–output coupling on the sensitivity of coupled resonator optical waveguide gyroscopes, *J. Opt. Soc. Am. B*, 2013, vol. 30, pp. 377–381.
7. Kalantarov, D. and Search, C.P., Effect of resonator losses on the sensitivity of coupled resonator optical waveguide gyroscopes, *Opt. Lett.*, 2014, vol. 39, no. 4, pp. 985–988.
8. Toland, J.R.E., Kaston, Z.A., Sorrentino, C., and Search, C.P., Chirped area coupled resonator optical waveguide gyroscope, *Opt. Lett.*, 2011, vol. 36, pp. 1221–1223.
9. Sorrentino, C., Toland, J., and Search, C.P., Ultra-sensitive chip scale Sagnac gyroscope based on periodically modulated coupling of a coupled resonator optical waveguide, *Opt. Express*, 2012, vol. 20, pp. 354–363.
10. Steinberg, B. Z., Scheuer, J., and Boag, A., Rotation-induced superstructure in slow-light waveguides with mode degeneracy: optical gyroscopes with exponential

sensitivity, *J. Opt. Soc. Am. B,* 2007, vol. 24, pp. 1216–1224.

11. Novitski, R., Steinberg, B.Z., and Scheuer, J., Losses in rotating degenerate cavities and a coupled-resonator optical-waveguide rotation sensor, *Phys. Rev. A*, 2012, vol. 85, p. 023813.
12. Scully, M. and Suhail Zubairy, M., *Quantum Optics*, Cambridge: Cambridge University Press 1997.
13. Ruffin, P.B., Fiber optics gyroscope sensors, in *Fiber Optic Sensors*, Yu, F.T.S., Yin, S., and Ruffin, P.B., Eds, CRC Press, 2008, 2nd edition.
14. Poon, J.K.S., Scheuer, J., Mookherjea, S., Paloczi, G.T., Huang, Y., and Yariv, A., Matrix analysis of microring coupled-resonator optical waveguides, *Opt. Express*, vol. 12, 2004, pp. 90–103.
15. Capmany, J., Munoz, P., Domenech, J.D., and Muriel, M.A., Apodized coupled resonator waveguides, *Opt. Express*, 2007, vol. 15, pp. 10196–10206.
16. Poon, J.K.S., Scheuer, J., Xu, Y., and Yariv, A., Designing coupled-resonator optical waveguide delay lines, *J. Opt. Soc. Am. B,* 2004, vol. 21, pp. 1665–1673.
17. Little, B.E., Chu, S.T., Haus, H.A., Foresi, J., and Laine, J.P., Microring resonator channel dropping filters, *J. Lightwave Technology*, 1997, vol. 15, pp. 998–1005.
18. Hah, D. and Zhang, D., Analysis of resonant optical gyroscopes with two input/output waveguides, *Opt. Express*, 2010, vol. 18, pp. 18200–18205.
19. Canciamilla, A., Torregiani, M., Ferrari, C., Morichetti, F., De La Rue, R.M., Samarelli, A., Sorel, M., and Melloni, A., Silicon coupled-ring resonator structures for slow light applications: potential, impairments and ultimate limits, *J. Opt.*, 2010, vol. 12, 104008.
20. Guillen-Torres, M.A., Cretu, E., Jaeger, N.A.F., and Chrostowski, L., Ring resonator optical gyroscopes-Parameter optimization and robustness analysis, *Journal of Lightwave Technology,* 2012, vol. 30, no. 12, pp. 1802–1817.
21. Morichetti, F., Ferrari, C., Canciamilla, A., and Melloni, A., The first decade of coupled resonator optical waveguides: bringing slow light to applications, *Laser & Photon. Rev.*, 2012, vol. 6, pp. 74–96.
22. Morichetti, F., Melloni, A., Ferrari, C., and Martinelli, M., Error-free continuously-tunable delay at 10 Gbit/s in a reconfigurable on-chip delay-line, *Opt. Express,* 2008, vol. 16, no. 12, pp. 8395–8405.
23. Xia, F., Sekaric, L., and Vlasov, Y., Ultracompact optical buffers on a silicon chip, *Nature Photon.*, 2007, vol. 1, pp. 65–71.
24. Gnan, M., Thorns, S., Macintyre, D.S., De La Rue, R.M., and Sorel, M., Fabrication of low-loss photonic wires in silicon-on-insulator using hydrogen silsesquioxane electron-beam resist, *Electronics Letters*, 2008, vol. 44, no. 2, pp. 115–116.
25. Morichetti, F., Melloni, A., Breda, A., Canciamilla, A., Ferrari, C., and Martinelli, M., A reconfigurable architecture for continuously variable optical slow-wave delay lines, *Opt. Express*, 2007, vol. 15, pp. 17273–17282.
26. Melloni, A., Costa, R., Monguzzi, P., and Martinelli, M., Ring-resonator filters in silicon oxynitride technology for dense wavelength-division multiplexing systems, *Opt. Lett.*, 2003, vol. 28, pp. 1567–1569.
27. Duchesne, D., Ferrera, M., Razzari, L., Morandotti, R., Little, B.E., Chu, S.T., and Moss, D.J., Efficient self-phase modulation in low loss, high index doped silica glass integrated waveguides, *Opt. Express*, 2009, vol. 17, no. 3, pp. 1865–1870.
28. Ferrera, M., Razzari, L., Duchesne, D., Morandotti, R., Yang, Z., Liscidini, M., Sipe, J.E., Chu, S., Little, B.E., and Moss, D.J., Low power continuous-wave nonlinear optics in doped silica glass integrated waveguide structures, *Nature Photonics*, 2008, vol. 2, no. 12, p. 737.
29. Little, B.E., Chu, S.T., Absil, P.P., Hryniewicz, J.V., Johnson, F.G., Seiferth, F., Gill, D., Van, V., King, O., and Trakalo, M., Very high order microring resonator filters for WDM applications, *IEEE Photonics Technology Letters*, 2004, vol. 16, no. 10, pp. 2263–2265.
30. Cooper, M.L., Gupta, G., Schneider, M.A., Green, W.M.J., Assefa, S., Xia, F., Vlasov, Y.A., and Mookherjea, S., Statistics of light transport in 235-ring silicon coupled-resonator optical waveguides, *Opt. Express,* 2010, vol. 18, pp. 26505–26516.
31. Melloni, A., Canciamilla, A., Ferrari, C., Morichetti, F., Faolain, L.O., Krauss, T.F., De La Rue, R., Samarelli, A., and Sorel, M., Tunable delay lines in silicon photonics: coupled resonators and photonic crystals, a comparison, *Photonics Journal, IEEE*, 2010, no. 2, pp. 181–194.